JOC The Journal of Organic Chemistry

ARTICLE

pubs.acs.org/joc

Self-Assembly and Gelation Behavior of Tris(phenylisoxazolyl)benzenes

Masahiro Tanaka,[†] Toshiaki Ikeda,[†] John Mack,[‡] Nagao Kobayashi,[‡] and Takeharu Haino*[,†]

[†]Department of Chemistry, Graduate School of Science, Hiroshima University, 1-3-1 Kagamiyama, Higashi-Hiroshima 739-8526, Japan

[‡]Department of Chemistry, Graduate School of Science, Tohoku University, Sendai 980-8578, Japan

Supporting Information

ABSTRACT: Low-molecular-mass organic gelators (LMOG), tris(phenylisoxazolyl)benzenes, were synthesized, and their self-assembling behavior was examined using ^{1}H NMR and UV−vis absorption spectroscopies. They turned into a gel in both nonpolar and highly polar solvents such as methylcyclohexane, ether, acetone, dimethylsulfoxide, etc. Field emission scanning electron microscopy (FESEM) observation of the xerogels of **1** and **3** possessing the saturated alkyl chains revealed that well-developed straight fibers were formed, whereas the unsaturated termini of the alkyl chains of **2** promoted the formation of both the right- and left-handed helical fibers. The self-association behavior of **1**, **2**, and **5** in solution were investigated using ^{1}H NMR and UV−vis spectroscopies. The flat aromatic compound **1** stacked in a columnar fashion along its C_3 axis via $\pi-\pi$ stacking interactions. The assemblies were regulated by the peripheral alkyl substituents; the saturated alkyl groups facilitated the assemblies while terminal double bonds impeded the intermolecular association, and the branched substituents obviously interfered in the formation of the stacks, probably due to steric requirements. Theoretical calculations suggest that the three dipoles of the isoxazole groups adopt the circular array. The conformational search of the hexameric stacks of **4** using MacroModel V9.1 gave rise to two major conformers: one is nonhelical and the other is helical. Further detailed structural analysis of the assemblies of chiral **5** using circular dichroism (CD) measurements indicated that their assemblies adopt helical structures in solution. CD spectra and DFT calculations revealed that *R*-**5** forms a left-handed supramolecular helicate. The coassembly of *R*- and *S*-**5** displayed chiral amplification, since the chiral information from **5** was transferred to the supramolecular chirality of the helical assemblies of **1**. A small amount of optically active **5** provided enough chiral stimulus to produce a remarkable chiral response and supramolecular helical structures of **1**.

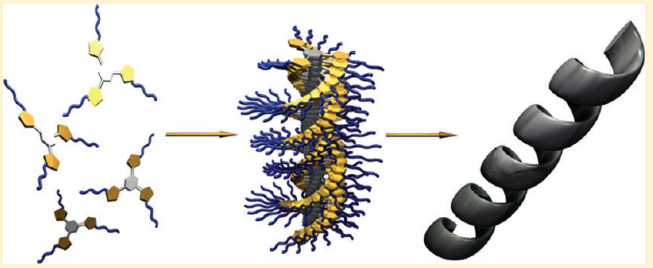

INTRODUCTION

Spontaneous self-assembly offers a powerful tool for the development of discrete, functional supramolecular nanostructures, starting from small and well-designed molecular components. Programmed noncovalent interactions hold together molecular components to define the direction and dimension of nanostructure formation. Numerous examples of supramolecular nanostructures through programed self-assembly have been reported to date, including nanorings, nanorods, stacks, and fibers.[1] Nanofibers, originating from the self-assembly of certain molecular components, have received extensive interest, since they offer versatile applications as "soft" materials. Molecular gels are a class of materials containing supramolecular fibrillar networks,[2] which entrap and immobilize solvent molecules in their voids. Amides,[3] ureas,[4] saccharides,[5] steroids,[6] polyaromatics,[1a,7] and perfluoroalkyl compounds[8] are known as low-molecular-weight organic gelators (LMOG) that produce the three-dimensional interconnected networks of well-defined fibers via self-assembly.[9]

π-Conjugated LMOG molecules are particularly intriguing because they assemble to produce photo- and electrochemically functional supramolecular assemblies.[10] The $\pi-\pi$ stacking interaction is strongly associated with the size of the conjugated aromatic surface; in fact, the more flat aromatic surface a π-conjugated molecule has, the more attractive interactions an assembly receives. A small aromatic molecule sometimes needs the aid of hydrogen bonding to create fibrous supramolecular assemblies.[11] Thus, a limited number of small aromatic gelators can assemble via stacking interactions to form fibrous supramolecular structures without the assistance of hydrogen bonds in organic solvents.[12]

Recently, we have found that a new class of low-molecular-weight gelators, tris(phenylisoxazolyl)benzenes **1** and **2**, capable of self-assembling in a helical fashion without the assistance of hydrogen bonds in solution,[13] and the introduction of azobenzene groups onto its periphery resulted in the photochromic regulation of gelation.[14] To design a rational molecular component that assembles to create a gel, it is essential to obtain an

Received: April 13, 2011
Published: May 12, 2011

insight into the molecular assembly process of the initial stage of gel formation. Herein we report a detailed account of the gelation and self-assembling behaviors of tris(phenylisoxazolyl)benzenes **1**−**5** (Figure 1).

RESULTS AND DISCUSSION

Synthesis. The synthesis of tris(phenylisoxazolyl)benzenes **1**−**5** is outlined in Scheme 1. 1,3-Dipolar cycloaddition of 1,3,5-triethynylbenzene and the corresponding nitriloxide prepared *in situ* from hydroximinoyl chlorides **6**−**10** by the treatment of triethylamine afforded the desired products **1**, **3**, **4**, **5**, and **11**. Deprotection of the TBS group of **11** with TBAF, followed by the ether formation, gave **2**. Compound **12** with the ethynyl groups instead of the isoxazole rings was prepared (Scheme 2). Sonogashira coupling of 1,3,5-tribromobenzene and (4-decyloxyphenyl)-ethyne smoothly proceeded to give **12**.

Gelation Property. The gelation tests of tris(phenylisoxazolyl)-benzenes **1**−**5** and tris(phenylethynyl)benzene **12** were performed using the "inverted test-tube method".[15] The compounds and solvents were placed into a screw-capped test tube and heated until the solid dissolved. The solution was then cooled to 298 K and left for 2 h under ambient conditions. The gelation was confirmed by the absence of the gravitational flow of solvents when the test tube was inverted (Table 1). The gels were thermoreversible and stable for at least 6 months at room temperature. Tris(phenlisoxazolyl)benzenes **1**−**3** possessing the alkoxy groups gelled in both polar and nonpolar solvents, whereas **4** and **5** were not gelators. Model compound **12** with the ethynyl groups instead of the isoxazole rings did not produce any gel. This indicates that the isoxazole rings play a key role in the formation of the gels.

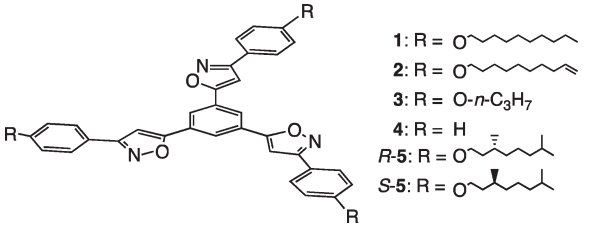

Figure 1. Tris(phenylisoxazlyl)benzene derivatives **1**−**5**.

Scheme 1. Synthesis of Tris(phenylisoxazlyl)benzene Derivatives 1−**5**

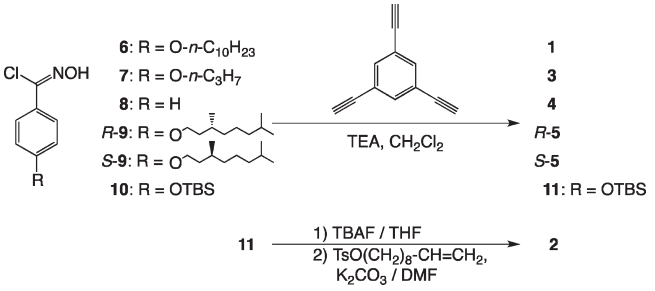

The gelation abilities of tris(phenylisoxazolyl)benzenes **1**−**3** are associated with the structures of their peripheral alkyl chains. The alkyl chain with the unsaturated termini reduces the gel stability (**1** vs **2**). The shorter alkyl chain of **3** is not effective for the gelation. The absence of a peripheral alkyl chain and branched chain structure remove the gelation abilities from the tris(phenylisoxazolyl)benzene (**4** and **5**).

Morphology of Gels. To gain a microscopic insight into the self-assembled structures of **1**−**3** in the organogels, the morphologies of their xerogels were observed using field emission scanning electron microscopy (FESEM). The FESEM images of the xerogels, prepared from the solution of **1** in acetone, displayed three-dimensional entangled networks, responsible for the gelation (Figure 2a). Figure 2b shows that the networks consist of the well-developed uniform straight fibers. Similar networks were

Table 1. Gelation Properties of 1−**5 and 12**[a,b,c]

solvent	1	2	3	4	5	12
hexane	P	P	I	I	P	S
cyclohexane	pG	P	I	I	P	S
methylcyclohexane	G (35)	P	I	I	P	S
benzene	S	S	G (30)	I	S	S
toluene	S	S	P	I	S	S
dichloromethane	S	S	S	S	S	S
chloroform	S	S	S	S	S	S
ether	G (18)	G (20)	I	I	P	S
acetone	G (8)	G (20)	G (25)	P	P	S
ethyl acetane	G (8)	P	P	I	S	S
acetonitrile	I	P	P	I	P	I
ethanol	I	I	I	I	P	I
IPA	I	I	I	I	P	I
THF	S	S	S	S	S	S
DMF	G (10)	G (20)	G (25)	S	P	S
DMSO	G (10)	G (20)	G (20)	S	pG	P

[a] G = gel, pG = partial gelation, P = precipitation, S = solution, and I = insoluble. [b] P, I, and S are at [gelator] = 20 mg mL^{-1}. [c] The critical gelation concentration (mg mL^{-1}) is shown in parentheses.

Scheme 2. Synthesis of Tris(phenyletynyl)benzene Derivative 12

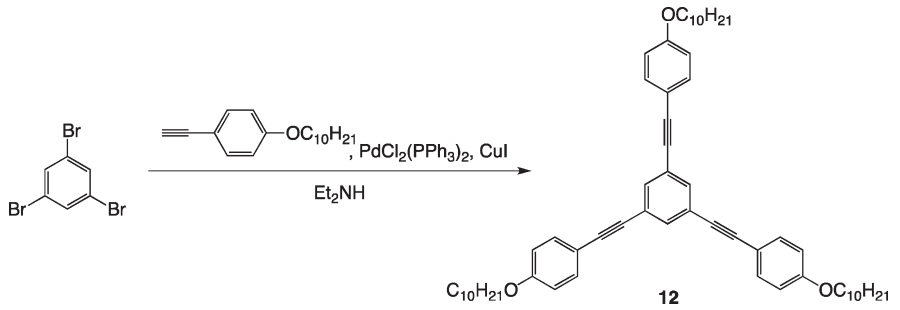

dx.doi.org/10.1021/jo200766u |J. Org. Chem. 2011, 76, 5082–5091

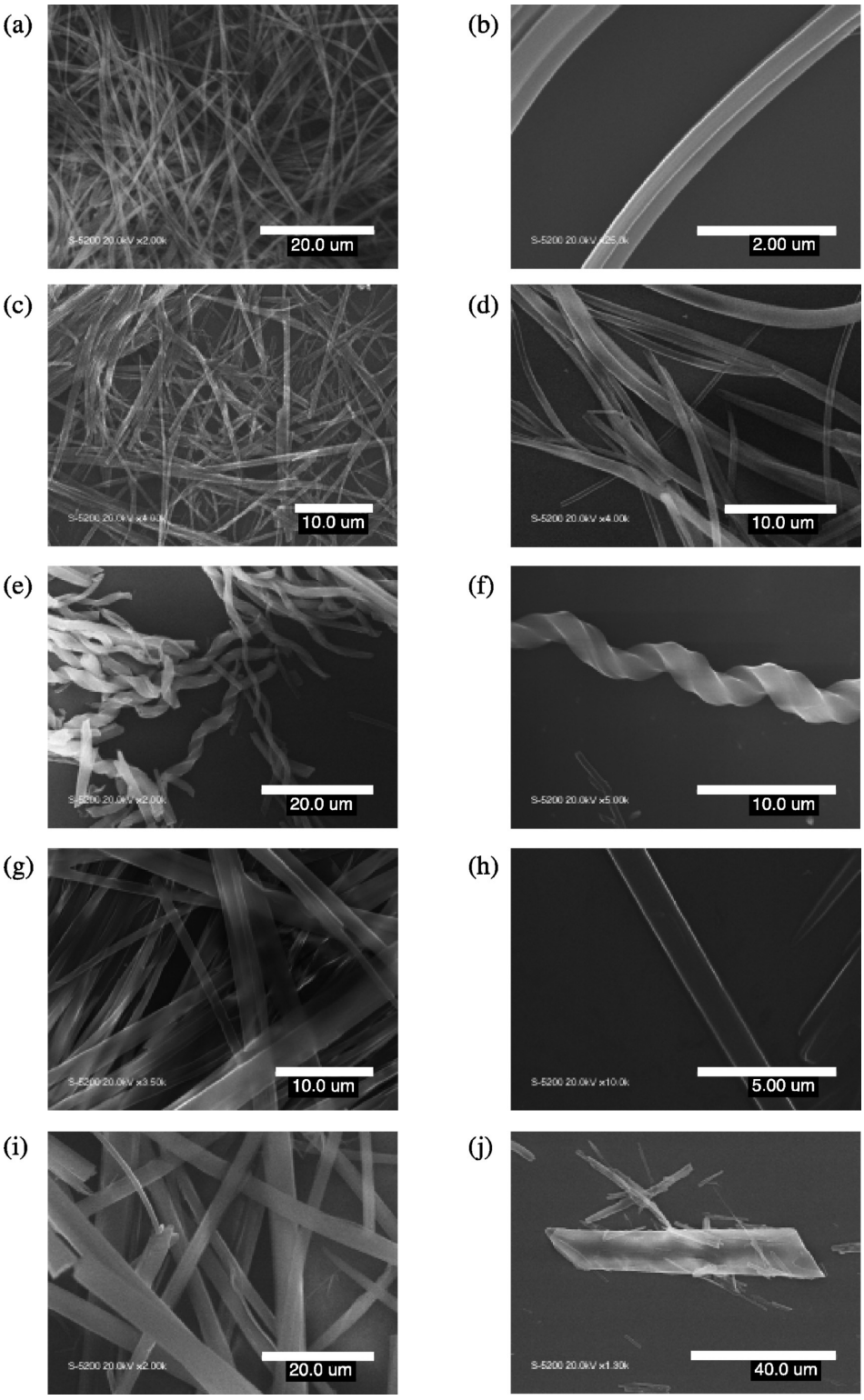

Figure 2. FESEM images of (a and b) the acetone xerogel of **1**; (c) the MCH xerogel of **1**; (d) the DMSO xerogel of **1**; (e and f) the DMSO xerogel of **2**; (g and h) the acetone xerogel of **2**; (i) the acetone xerogel of **3**; (j) **5**.

observed for the xerogels of **1**, obtained from solutions using methylcyclohexane (MCH) and DMSO (Figure 2c and d). A slight structural change in the side chains of **1** leads to a large difference in terms of the morphologies of the gels. Figure 2e−h display that the morphologies for the assembly of **2** having the unsaturated termini of the alkyl chains revealed that both the right- and left-handed helical fibers formed from the solution in DMSO (Figure 2e and f),[16] whereas the straight fibers were obtained from the acetone solution (Figure 2g and h). The assembly of **3** generated the straight fibers with a diameter of a

dx.doi.org/10.1021/jo200766u |*J. Org. Chem.* 2011, 76, 5082–5091

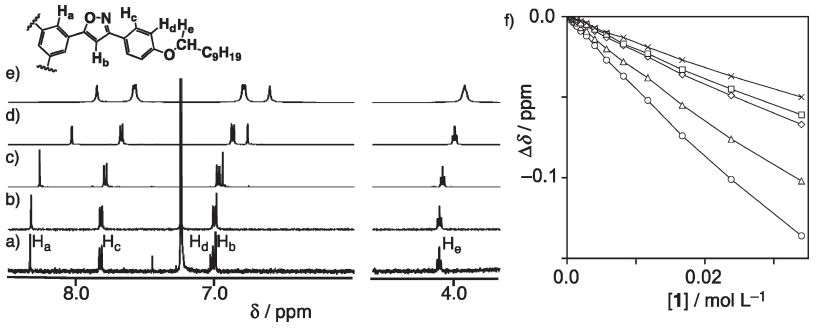

Figure 3. ^{1}H NMR spectra (left) of **1** in the concentrations of (a) 0.163, (b) 1.98, (c) 16.8, (d) 100, and (e) 200 mmol L^{-1} at 298 K in chloroform-d_1. Plots (right) of the concentrations of **1** vs chemical shift changes of the protons: (○) H_a; (△) H_b; (◇) H_c; (□) H_d; and (×) H_e.

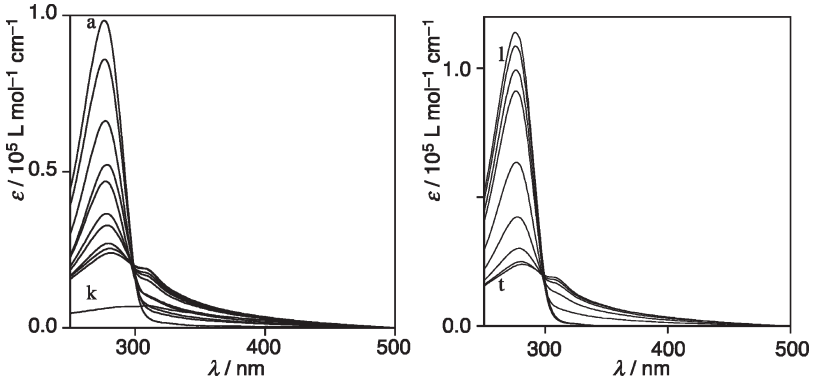

Figure 4. UV−vis absorption spectra of **1** (left at 293 K) and (right, [**1**] = 50.0 μmol L^{-1}) in MCH. The concentrations of **1** (left) are from the top (curves a−k) 1.0, 2.5, 5.0, 7.5, 10.0, 15.0, 20.0, 30.0, 40.0, 50.0, and 1000.0 μmol L^{-1}. The temperatures of the solution of **1** (right) are from the top (curves l−t) 333, 328, 323, 318, 313, 308, 303, 298, and 293 K.

few micrometers (Figure 2i). The size of the fibers was about 10 times thicker than that of **1**. On the other hand, microcrystals were obtained from the chiral molecule **5**, which did not form any stable gel (Figure 2j).

Self-Association Behavior. In the initial stage of gel formation, molecular association events of LMOGs promote anisotropic assembly that defines the direction and dimension of gel growth. Thus, the molecular structure of LMOGs directly influences the gel morphology and results in fibers, ribbons, or sheets. A detailed analysis of molecular association of LMOGs should give an insight into the mechanism of gel formation at the molecular level.

The self-assembling behavior of **1** was examined using ^{1}H NMR and UV−vis spectroscopies. The ^{1}H NMR signals of **1** were concentration-dependent in chloroform-d_1; most of the aromatic signals shifted upfield upon increasing the concentrations of **1** (Figure 3). This indicates that **1** forms stacked assemblies in which the aromatic protons are placed in the shielding regions produced by the neighboring aromatic rings, whereas the aromatic protons of **12** were independent of concentration. These observations indicate that the isoxazole ring is indispensable to drive the supramolecular assembly.

The plots of the chemical shift changes of the protons vs the concentrations of **1** gave hyperbolic curves (Figure 3). Nonlinear curve-fitting analysis based on the isodesmic model[17,18] produced the estimated complexation-induced shifts (H_a: −1.34, H_b: −1.10, H_c: −0.80, H_d: −0.59 ppm) with the association constant (K_E) of 3.7 ± 0.3 L mol^{-1}. The complexation-induced shifts decreased upon increasing the distance of the protons from the C_3 axis of **1**. This can be attributed to the columnar nature of the self-assembled structures, in which **1** stacks along its C_3 axis producing anisotropic growth.

The formation of large stacked assemblies of **1** was confirmed by UV−vis absorption spectroscopy in methylcyclohexane (MCH) (Figure 4). A dilute solution (1 μmol L^{-1}) of **1** displayed a sharp absorption band at 278 nm in MCH. The absorption band decreased upon increasing its concentrations, and then a new broad band gradually emerged at approximately 310 nm. When the concentration of **1** reached 1.0 mmol L^{-1}, the solution became stained and gave a broad band with a peak at 310 nm. The UV−vis absorption spectra of **1** (50 μmol L^{-1}) were also sensitive to temperature. The spectrum at 293 K had two peaks at 278 and 310 nm, respectively. Upon warming the solution to 323 K, the broad band at 310 nm diminished, and the peak at 278 nm intensified. It is accepted that supramolecular assemblies formed via noncovalent interactions tend to dissociate upon warming or dilution of the solution, because they have to pay a large entropic cost to preserve the assembled state. The red shift of the absorption band from 278 to 310 nm indicates that the supramolecular association of **1** produces *J*-type assemblies and that **1** equilibrates with its stacked assemblies.[19]

The structure of the peripheral alkyl chains of the tris(phenylisoxazolyl)benzenes can influence their intermolecular association. Therefore, introduction of the unsaturated bond and the branched structure onto the peripheral alkyl chains should alter the association.[20] To investigate the influence of the structural

dx.doi.org/10.1021/jo200766u |*J. Org. Chem.* 2011, 76, 5082–5091

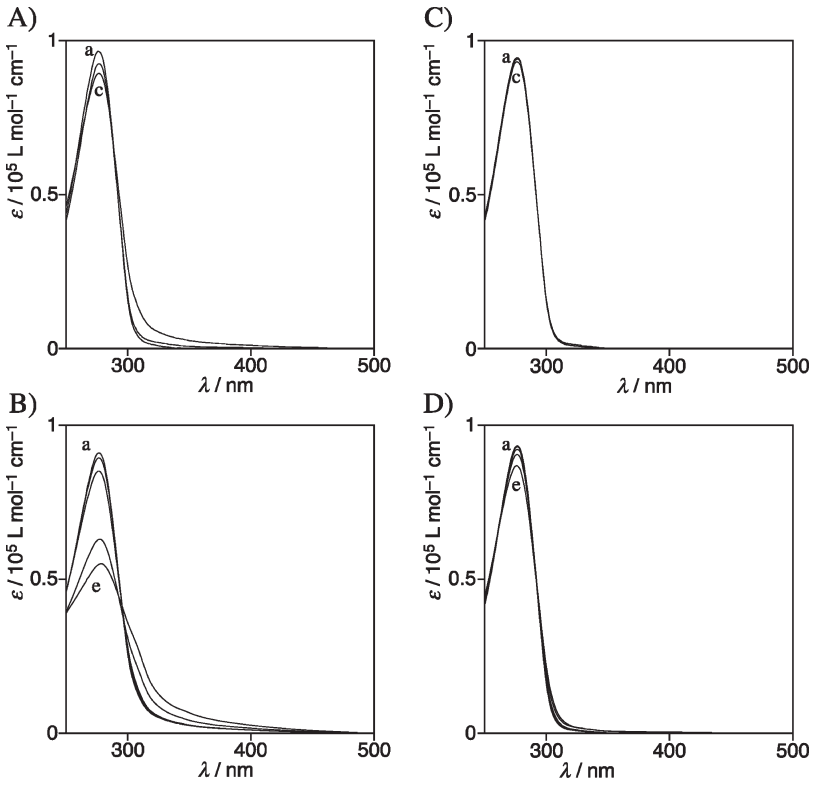

Figure 5. UV−vis spectra of **2** (A and B) and **5** (C and D) in MCH. (A) [**2**] = (a) 1.0, (b) 10.0, and (c) 100.0 μmol L^{-1} at 293 K. (B) [**2**] = 50.0 μmol L^{-1}; T = (a) 298, (b) 293, (c) 288, (d) 283, and (e) 278 K. (C) [**5**] = (a) 1.0, (b) 10.0, and (c) 100.0 μmol L^{-1} at 293 K. (D) [**5**] = 50.0 μmol L^{-1}; T = (a) 298, (b) 293, (c) 288, (d) 283, and (e) 278 K.

differences of the chains on the self-assembly, we attempted to determine the association constants of compounds **2** and **5** using UV−vis absorption spectroscopy in MCH; however, the association constants were too small to be determined accurately. The relative binding abilities among **1**, **2**, and **5** can be qualitatively evaluated by a comparison of the concentration and temperature dependence of their UV−vis absorption spectra. The absorption spectra of **2** and **5** were obviously less sensitive to concentration changes than those of **1**, but **2** showed slightly greater spectral changes than **5** (Figure 5A and C). Upon cooling the solutions of **2** and **5** from 298 to 278 K, their spectra gave rise to the contrastive difference (Figure 5B and D). At 298 K, the value of the molar extinction coefficient of **2** at 278 nm was close to that of **5**, indicating that **2** and **5** are mainly present as a monomer. On cooling the solution to 278 K, the molar extinction coefficient of **2** at 278 nm diminished, and a broad band at around 310 nm emerged and is ascribed to the assembly. It is clear that a fair amount of the assembly of **2** is produced at the low temperature. The relative stability of these assemblies were qualitatively determined, and are in the order of **1** > **2** > **5** (Figures 4 and 5).[21] Therefore, unsaturation and the branches[22] of the alkyl termini reduce the intermolecular association considerably.

Thermodynamic Studies. The NMR and UV−vis dilution studies provided the estimated association constants of **1** in three different solvent systems (Table 2). In both MCH and dimethylsulfoxide (DMSO), the value is very large compared with that in chloroform. To gain an insight into the self-assembly of **1** in a variety of solvents, the enthalpic and entropic contributions for the association were determined. The van't Hoff plots gave the thermodynamic parameters for the self-association.

Table 2. Association Constants at 293 K and Thermodynamic Parameters of Self-Association of 1

solvent	K_E (L mol^{-1})	ΔH (kcal mol^{-1})	ΔS (cal mol^{-1} K^{-1})
MCH[a]	(1.0 ± 0.1) × 10^5	−15 ± 1	−29 ± 6
$CDCl_3$[b]	3.7 ± 0.3	−2.50 ± 0.09	−5.8 ± 0.3
DMSO[a]	(4.4 ± 0.1) × 10^5	−10 ± 2	−9 ± 7

[a] Determined on the basis of the infinite association model by the UV−vis method. [b] Determined on the basis of the infinite association model by the NMR method.

The self-association process is enthalpy-driven and entropy-opposed. This is commonly observed for a multiple molecular association. MCH and DMSO are good solvents for the gel formation; the self-association of **1** gained enthalpic contributions larger than that in chloroform. The enthalpic contributions are involved in desolvation and attractive intermolecular forces, including $\pi-\pi$ stacking, dipole−dipole, and van der Waals interactions. A well-solvated molecule commonly receives small enthalpic contribution during its association, because the desolvation of the molecule has to pay a large enthalpic cost. This rationalizes the large enthalpic difference observed among the solvents; in fact, **1** is very soluble in chloroform but less soluble in the other solvents.

Molecular Modeling. Theoretical calculation of the molecular assembly gives a plausible picture that complements the experimental studies in solution. 1,3,5-Tris[3-(4-methoxyphenyl)-isoxazol-5-yl]benzene (**13**) and its partial structure, 3-(4-methoxyphenyl)-5-phenylisoxazole (**14**), were subjected to theoretical

dx.doi.org/10.1021/jo200766u |*J. Org. Chem.* 2011, 76, 5082–5091

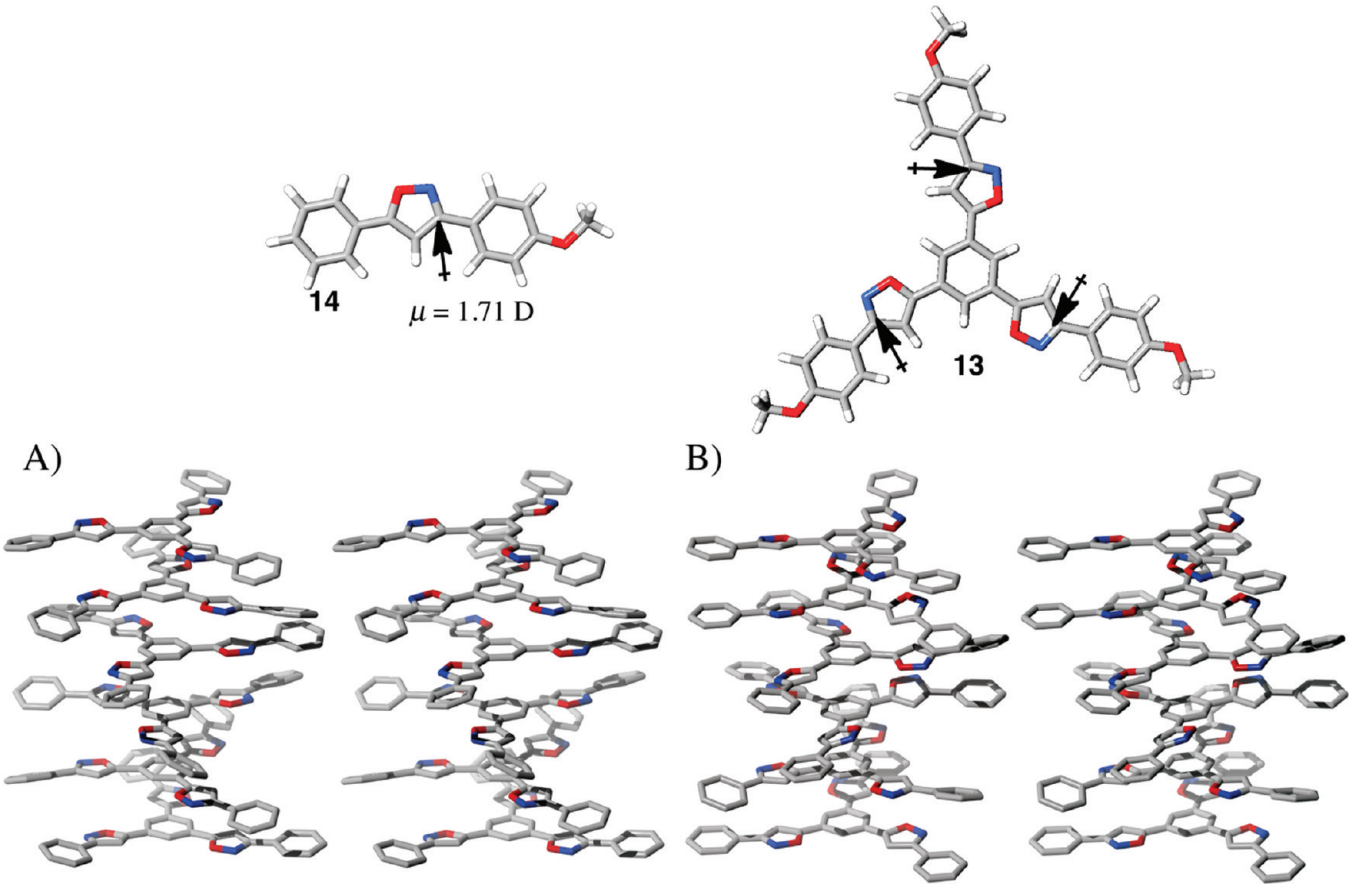

Figure 6. Calculated geometries of **13** and its partial structure **14** by DFT method using B3LYP/6-31G*. Stereo plots of two local minimum geometries for the hexameric **4** obtained from conformation search by MacroModel program: (A) helical arrangement of the local dipoles and (B) anti parallel arrangement of them.

calculations using the DFT method (B3LYP/6-31G*).[22] Compound **14** has a fairly large dipole moment (μ = 1.71 D), directed to the nitrogen atom along the N=C double bond. The local dipole−dipole interactions among the three isoxazole rings of **13** enable them to adopt a circular array (Figure 6);[12c,d] in fact, flipping one of the isoxazole rings to the opposite direction gives rise to an increase in the total energy (ΔE = 1.00 kcal mol^{-1}). The intramolecular circular array of the three dipole moments, of course, regulates the intermolecular arrangement of the supramolecular self-assembly.

To obtain plausible structures of the supramolecular self-assemblies, a conformational study of the hexameric assembly of **4** was performed as a model system with the low mode sampling method[23] using MMFF94s as implemented in MacroModel V.9.1.[24] During the calculation, the C_3 axes of the six molecules were constrained along the principal anisotropic axis to ensure that each molecular center did not slip out of the principal axis. Two major geometries (Figure 6A and B) were obtained within 1.0 kcal mol^{-1}. Conformer A adopts a helical geometry; the local dipoles align in a head-to-tail manner. In conformer B, the phenylisoxazolyl groups of **4** adopt an unusually eclipsed geometry due to the attractive antiparallel orientation of the local dipoles; the eclipsed arrangement produces molecular pairs, built up as piles in a staggered manner. Hence, conformer B is achiral. While the two conformers can exist in solution, the presence of chiral conformer A leads to a chiral environment where the helical sense of conformer A can be biased by the addition of chiral stimuli.

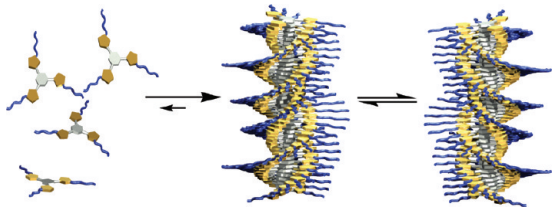

Figure 7. Schematic representation of the formation of the helicate and its equilibrium between right- and left-handed helical conformations.

Chiral Induction in Supramolecular Assembly. These calculations suggest that the tris(phenylisoxazoly)benzene can form helical columnar assemblies. Generally, in the absence of a chiral source, the helical assemblies have both possible right- and left-handed helical conformations, having equal intermolecular interaction energies; thus, the helical assemblies exist as racemic mixtures of two enantiomers (Figure 7). Upon the introduction of a chiral source, the equilibrium between the right- and left-handed helical conformations can be biased in the higher level of organization, because the relationships between the two conformations change from enantiomer to diastereomer. The helical assemblies, formed from chiral molecules, produce induced circular dichroism.[16,21,25]

dx.doi.org/10.1021/jo200766u |*J. Org. Chem.* 2011, 76, 5082–5091

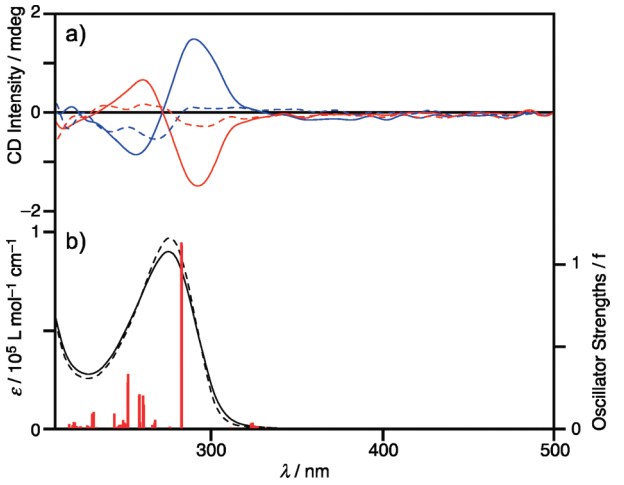

Figure 8. (a) Temperature-dependent CD spectra of *R*-**5** (red) and *S*-**5** (blue) in the concentrations of 150 μmol L^{-1} in cyclohexane at 293 K (dashed line) and 283 K (solid line). All CD spectra were recorded in a 1 × 10 × 45 mm^3 quartz cell. (b) Temperature-dependent UV spectra of *R*-**5** at 293 K (dashed line) and 283 K (solid line) in the concentrations of 150 μmol L^{-1} in cyclohexane. A gas-phase TDDFT calculation for model compound **13** based on a B3LYP geometry optimization with 6-31(d) basis sets.

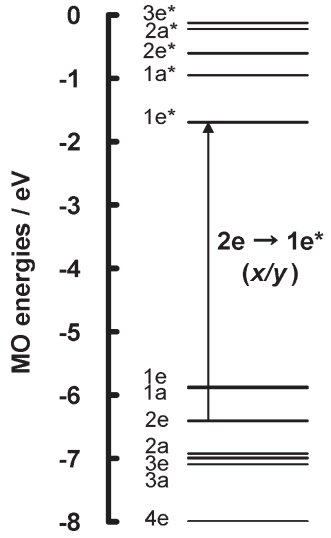

Figure 9. MO energy diagram derived from a B3LYP geometry optimization of TDDFT-**5**. The main band in the TDDFT calculated spectrum at 283 nm is predicted to arise from the *x*/*y*-polarized 2e → 1e* one-electron transition.

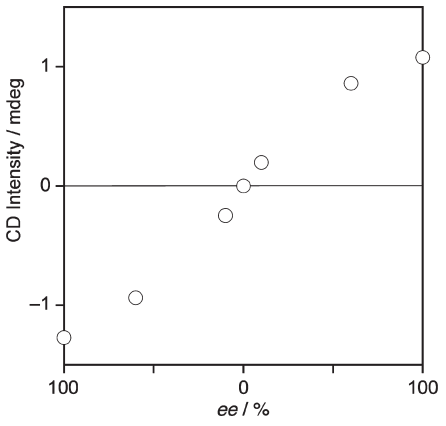

Figure 10. Intensity change of CD band at 290 nm by varying the molar ratio of *R*-**5** and *S*-**5** at 283 K in the concentration of 100 μmol L^{-1} in cyclohexanene.

Figure 8 contains the UV−vis absorption and CD spectra of **5** in cyclohexane. An intense peak is observed in the absorption spectrum at 278 nm. The peak decreases, and the new broad band emerges at approximately 310 nm when the temperature is lowered from 293 to 283 K with isosbestic points observed at 259 and 293 nm, which correspond to those found in MCH (Figure 5D). This indicates that there is a direct change between two states. The CD spectra of *R*-**5** and *S*-**5** exhibit a mirror image relationship with respect to the line of $[\theta]$ = 0. When the temperature is lowered from 293 to 283 K, the signals intensify and clear S−shaped curves are observed at 278 nm. The CD spectra at 293 K are weak, and the dispersion curves are not consistent with the pattern that would be normally expected for exciton coupling. This suggests that monomeric compounds predominate in solution. When the temperature is lowered, the signal intensifies and shifts to shorter wavelength. The intensification and blue shift of the inflection point are consistent with cofacial-type aggregation. The minus-to-plus pattern observed in ascending energy terms in the CD spectrum of *R*-**5** indicates that the *R*-**5** dimer forms a left-handed helix.[25] Conversely, the plus-to-minus pattern observed in the *S*-**5** dimer spectrum is consistent with a right-handed helix. The most intense band in the calculated TDDFT spectrum lies at 283 nm,[22] Figure 8, in excellent agreement with the experimental data, and is predicted to arise primarily from an *x*/*y*−polarized 2e → 1e* transition (Figure 9).

Intriguingly, chiral amplification was observed in the association of **5**. Plotting the intensity of the CD band at 290 nm versus the enantiomeric excess of **5** gave rise to nonlinear response (Figure 10). If the helical assemblies were formed from homochiral molecules and cooperative interactions did not exist between the assemblies, the plots would produce a linear correlation. The nonlinear response indicates that two enantiomers of *R*-**5** and *S*-**5** coassemble to form helical assemblies, and their helical directions have a tendency to depend on the major enantiomer. This is the so-called "Majority Rule",[26] which is usually observed in chiral polymerization[27] but rarely found in supramolecular assembly.[28]

If the "Sergeants-and-Soldiers principle"[29] is operative in the dynamic structures (*P* and *M*) of the helical assemblies of **1**, by means of the presence of a chiral source, the chemical equilibrium between *P* and *M* conformations can be biased in the higher supramolecular level of organization. CD spectra of only achiral **1** was silent and chiral **5** gave rise to a very weak Cotton effect at the same concentration as **1** due to weak association (Figure 11). Upon the addition to 0.01 mol % *R*-**5** or *S*-**5** to the solution of **1**, a mirrored and strong Cotton effect was observed. It is remarkable that the supramolecular assembly demonstrates the unusual optical activity in the CD spectrum even in the presence of only 0.01 mol % of chiral source **5**. The chiral information from the chiral sources is transcripted and magnified by the self-assembled columnar assemblies.

dx.doi.org/10.1021/jo200766u |*J. Org. Chem.* 2011, 76, 5082–5091

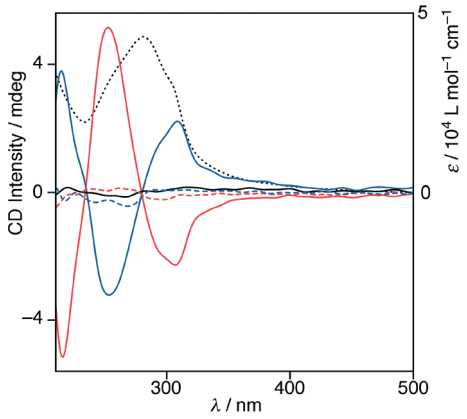

Figure 11. CD spectra of **1** (solid black line, c_t = 100 μmol L^{-1}), *R*-**5** (dashed red line, c_t = 100 μmol L^{-1}), *S*-**5** (dashed blue line, c_t = 100 μmol L^{-1}), **1** (c_t = 100 μmol L^{-1}) with 0.01 mol % *R*-**5** (solid red line), **1** (c_t = 100 μmol L^{-1}) with 0.01 mol % *S*-**5** (solid blue line), and absorption spectrum of **1** (dashed black line) at 293 K in cyclohexane. All CD spectra were recorded in a 1 × 10 × 45 mm^3 quartz cell.

CONCLUSION

We have demonstrated that tris(phenylisoxazolyl)benzenes **1**−**3** assemble and produce a gel in polar and nonpolar solvents; the unique chiral response originates from the helical supramolecular assembly driven by dipole−dipole and $\pi-\pi$ stacking interactions. The gelation abilities of the tris(phenylisoxazolyl)-benzenes are associated with the stabilities of their assemblies. Quantitative studies of the assemblies using an isodesmic association model reveals that the solvent properties and the steric interaction of the peripheral alkyl chains influence the stabilities. A detailed picture of the supramolecular assemblies was revealed using theoretical calculations. Achiral and helical supramolecular assemblies exist, and the latter is responsible for the chiral response. The chiral supramolecular assembly forms right- and left-handed helical conformations both in the gel and in solution. The coassembly of *R*- and *S*-**5** leads to chiral amplification. The helical structures are influenced by an extremely tiny proportion of chiral monomer. The "Majority Rule" and "Sergeants-and-Soldiers principle" operate in the dynamic helical assembly.

EXPERIMENTAL SECTION

1,3,5-Tris[3-(4-decyloxyphenyl)isoxazol-5-yl]benzene 1. To a solution of 1,3,5-triethynylbenzene (446 mg, 2.97 mmol) and benzohydroximoyl chloride **6**[30] (3.20 g, 9.82 mmol) in CH_2Cl_2 (60 mL) was added triethylamine (2.48 mL, 17.8 mmol). After stirring at room temperature for 48 h, the reaction mixture was concentrated. The crude product was purified by column chromatography on silica gel ($CHCl_3$) to give **1** (2.32 g, 80%) as a white solid. Mp 132−133 °C; ^{1}H NMR (500 MHz, 10 mM, $CDCl_3$) δ 8.30 (s, 3H), 7.82 (d, J = 8.9 Hz, 6H), 7.00 (d, J = 8.9 Hz, 6H), 6.97 (s, 3H), 4.02 (t, J = 6.7 Hz, 6H), 1.79−1.85 (m, 6H), 1.45−1.51 (m, 6H), 1.29−1.38 (m, 36H), 0.89 (t, J = 6.8 Hz, 9H); ^{13}C NMR (125 MHz, 10 mM, $CDCl_3$) δ 168.1, 162.9, 160.9, 129.3, 128.3, 123.9, 120.9, 115.0, 98.8, 68.2, 31.9, 29.6 × 2, 29.4, 29.3, 29.2, 26.0, 22.7, 14.1; IR (KBr) 3110, 2920, 2849, 1612, 1561, 1526, 1469, 1435, 1388, 1299, 1290, 1255, 1175, 1114, 1020 cm^{-1}; HRMS (FAB$^+$) calcd for $C_{63}H_{82}N_3O_6$ 976.6204 [M + H]$^+$, found 976.6183. Anal. Calcd for $C_{63}H_{81}N_3O_6$: C 77.50, H 8.36; N 4.30. Found: C 77.57, H 8.33, N 4.68.

1,3,5-Tris[3-(4-propyloxyphenyl)isoxazol-5-yl]benzene 3. To a solution of 1,3,5-triethynylbenzene (271 mg, 1.80 mmol), and benzohydroximoyl chloride **7**[30] (1.38 g, 6.48 mmol) in CH_2Cl_2 (20 mL) was added triethylamine (1.5 mL, 10.8 mmol). After stirring at room temperature for 48 h, the reaction mixture was concentrated. The crude product was purified by column chromatography on silica gel ($CHCl_3$) and recrystallized from toluene solution to give **3** (689 mg, 62%) as a white solid. Mp 172−174 °C; ^{1}H NMR (500 MHz, 10 mM, $CDCl_3$) δ 8.30 (s, 3H), 7.82 (d, J = 9.0 Hz, 6H), 7.01 (d, J = 9.0 Hz, 6H), 6.98 (s, 3H), 3.99 (t, J = 6.5 Hz, 6H), 1.82−1.88 (m, 6H), 1.07 (t, J = 7.0 Hz, 9H); ^{13}C NMR (125 MHz, 10 mM, $CDCl_3$) δ 168.1, 162.9, 160.8, 129.3, 128.2, 123.9, 120.9, 114.9, 98.8, 69.6, 22.5, 10.5; IR (KBr) 2964, 2934, 2876, 1612, 1561, 1525, 1467, 1433, 1387, 1294, 1257, 1175, 1117, 1065, 1046, 1017 cm^{-1}; HRMS (FAB$^+$) calcd for $C_{42}H_{40}N_3O_6$ 682.2917 [M + H]$^+$, found 682.2916. Anal. Calcd for $C_{42}H_{39}N_3O_6$: C 73.99, H 5.77, N 6.16. Found: C 73.76, H 5.83, N 5.99.

1,3,5-Tris(3-phenylisoxazol-5-yl)benzene 4. To a solution of 1,3,5-triethynylbenzene (79 mg, 0.53 mmol), and benzohydroximoyl chloride **8**[31] (297 mg, 1.9 mmol) in CH_2Cl_2 (5 mL) was added triethylamine (1.5 mL, 10.8 mmol). After stirring at room temperature for 48 h, the reaction mixture was concentrated. The crude product was purified by column chromatography on silica gel ($CHCl_3$) to give **4** (88 mg, 33%) as a white solid. Mp > 300 °C; ^{1}H NMR (500 MHz, 1 mM, $CDCl_3$) δ 8.39 (s, 3H), 7.92−7.94 (m, 6H), 7.52−7.54 (m, 9H), 7.09 (s, 3H); ^{13}C NMR (75 MHz, $CDCl_3$) δ 168.5, 163.5, 130.5, 129.4, 129.2, 128.8, 127.1, 124.3, 99.3; IR (KBr) 3104, 3051, 1625, 1593, 1561, 1509, 1469, 1450, 1394, 1284, 1253, 1092, 1117 cm^{-1}; HRMS (FAB$^+$) calcd for $C_{33}H_{22}N_3O_3$ 508.1661 [M + H]$^+$, found 508.1675. Anal. Calcd for $C_{33}H_{21}N_3O_3 \cdot 0.5H_2O$: C 76.73, H 4.29, N 8.13. Found: C 76.92, H 4.10, N 8.07.

***(R)*-4-(3,7-Dimethyloctoxy)benzaldoxime.** To a solution of (*R*)-4-(3,7-dimethyloctoxy)benzaldehyde (2.94 g, 11.2 mmol) in ethanol (20 mL) and water (10 mL) was added hydroxylamine hydrochloride (820 mg, 11.8 mmol). Then, NaOH (1.12 g, 28.0 mmol) in water (10 mL) was added slowly. The reaction mixture was stirred at room temperature for 1 h and was quenched with 6 N HCl. The resulting solution was extracted with ether, dried over Na_2SO_4, and concentrated to give the benzaldoxime (2.94 g, 95%) as a white solid. Mp 30−33 °C; $[\alpha]^{25}_D$ = +4.7 cm^3 g^{-1} dm^{-1} (c 0.39 g cm^{-3} in chloroform); ^{1}H NMR (300 MHz, $CDCl_3$) δ 8.08 (s, 1H), 7.66 (s, 1H), 7.50 (d, J = 8.7 Hz, 2H), 6.90 (d, J = 8.7 Hz, 2H), 3.96−4.07 (m, 2H), 1.06−1.88 (m, 10H), 0.94 (d, J = 6.6 Hz, 3H), 0.87 (d, J = 6.6 Hz, 6H); ^{13}C NMR (75 MHz, $CDCl_3$) δ 160.6, 150.1, 128.4, 124.4, 114.7, 66.4, 39.2, 37.3, 36.1, 29.8, 28.0, 24.6, 22.7, 22.6, 19.6; IR (KBr) 3282, 2955, 2925, 2870, 1607, 1575, 1515, 1468, 1420, 1383, 1365, 1305, 1252, 1173, 1111, 1053, 1014 cm^{-1}; HRMS (FAB$^+$) calcd for $C_{17}H_{28}NO_2$ [M + H$^+$] 278.2120, found 278.2113. Anal. Calcd for $C_{17}H_{27}NO_2$: C, 73.61; H, 9.81; N, 5.05. Found: C, 74.19; H, 9.70; N, 5.05.

***(S)*-4-(3,7-Dimethyloctoxy)benzaldoxime.** To a solution of (*S*)-4-(3,7-dimethyloctoxy)benzaldehyde (2.35 g, 8.96 mmol) in ethanol (20 mL) and water (10 mL) was added hydroxylamine hydrochloride (685 mg, 9.86 mmol). Then, NaOH (896 mg, 22.4 mmol) in water (5 mL) was added slowly. The reaction mixture was stirred at room temperature for 1 h and was quenched with 6 N HCl. The resulting solution was extracted with ether, dried over Na_2SO_4, and concentrated to give the benzaldoxime (1.80 g, 72%). Mp 30−32 °C; $[\alpha]^{25}_D$ = −4.5 cm^3 g^{-1}dm^{-1} (c 0.43 g cm^{-3} in chloroform); ^{1}H NMR (300 MHz, $CDCl_3$) δ 8.08 (s, 1H), 7.50 (d, J = 8.7 Hz, 2H), 7.30 (s, 1H), 6.89 (d, J = 8.7 Hz, 2H), 3.95−4.07 (m, 2H), 1.08−1.89 (m, 10H), 0.94 (d, J = 6.6 Hz, 3H), 0.87 (d, J = 6.6 Hz, 6H); ^{13}C NMR (75 MHz, $CDCl_3$) δ 160.6, 150.1, 128.4, 124.4, 114.7, 66.4, 39.2, 37.3, 36.1, 29.8, 28.0, 24.6, 22.7, 22.6, 19.6; IR (KBr) 3285, 2954, 2927, 2870, 1607, 1575, 1515, 1469, 1420, 1384, 1365, 1305, 1252, 1173, 1111, 1051, 1016 cm^{-1}; HRMS (FAB$^+$) calcd for $C_{17}H_{28}NO_2$ [M + H$^+$] 278.2120, found 278.2101. Anal. Calcd for $C_{17}H_{27}NO_2$: C, 73.61; H, 9.81; N, 5.05. Found: C, 73.63; H, 9.80; N, 4.97.

dx.doi.org/10.1021/jo200766u |*J. Org. Chem.* 2011, 76, 5082–5091

(*R*)-4-(3,7-Dimethyloctoxy)benzohydroximoyl Chloride *R*-9. To a solution of (R) −4-(3,7-dimethyloctoxy)benzaldoxime (2.02 g, 7.28 mmol) in DMF (8 mL) at 0 °C was added *N*-chlorosuccinimide (1.02 g, 7.64 mmol). After stirring at room temperature for 1 h, the reaction mixture was poured into four volumes of water and extracted with ether. The organic layer was washed three times with water, dried over $NaSO_4$, and concentrated to give *R*-**9** (2.20 g, 97%). The product prepared in this manner did not require further purification for conversion to the isoxazole. ^{1}H NMR (300 MHz, $CDCl_3$) δ 7.76 (d, J = 9.0 Hz, 2H), 6.90 (d, J = 9.0 Hz, 2H), 3.97−4.10 (m, 2H), 1.11−1.89 (m, 10H), 0.94 (d, J = 6.6 Hz, 3H), 0.87 (d, J = 6.6 Hz, 6H).

(*S*)-4-(3,7-Dimethyloctoxy)benzohydroximoyl Chloride *S*-9. To a solution of (*S*)- 4-(3,7-dimethyloctoxy)benzaldoxime (1.62 g, 5.84 mmol) in DMF (6 mL) at 0 °C was added *N*-chlorosuccinimide (858 mg, 6.43 mmol). After stirring at room temperature for 1 h, the reaction mixture was poured into four volumes of water and extracted with ether. The organic layer was washed three times with water, dried over $NaSO_4$, and concentrated to give *S*-**9** (1.82 g, 99%). The product prepared in this manner did not require further purification for conversion to the isoxazoles. ^{1}H NMR (300 MHz, $CDCl_3$) δ 7.76 (d, J = 9.0 Hz, 2H), 6.90 (d, J = 9.0 Hz, 2H), 3.97−4.10 (m, 2H), 1.11−1.89 (m, 10H), 0.94 (d, J = 6.6 Hz, 3H), 0.87 (d, J = 6.6 Hz, 6H).

1,3,5-Tris{3-[(*R*)-4-(3,7-dimethyloctoxy)phenyl]isoxazol-5-yl}benzene *R*-5. To a solution of 1,3,5-triethynylbenzene (305 mg, 2.03 mmol) and benzohydroximoyl chloride *R*-**9** (2.20 g, 7.05 mmol) in CH_2Cl_2 (50 mL) was added triethylamine (2.8 mL, 20 mmol). After being stirred at room temperature for 48 h, the reaction mixture was concentrated. The crude product was purified by column chromatography on silica gel ($CHCl_3$) to give *R*-**5** (675 mg, 34%) as a white solid. Mp 140−141 °C; $[\alpha]^{25}_D$ = +5.5 $cm^3\ g^{-1}\ dm^{-1}$ (c 1.0 g cm^{-3} in chloroform); ^{1}H NMR (300 MHz, 10 mM, $CDCl_3$) δ 8.31 (s, 3H), 7.82 (d, J = 9.0 Hz, 6H), 7.01 (d, J = 9.0 Hz, 6H), 6.99 (s, 3H), 4.00−4.12 (m, 6H), 1.14−1.90 (m, 30H), 0.97 (d, J = 6.6 Hz, 9H), 0.88 (d, J = 6.6 Hz, 18H); ^{13}C NMR (75 MHz, 10 mM, $CDCl_3$) δ 168.1, 162.9, 160.8, 129.2, 128.2 123.9, 120.8, 114.9, 98.8, 66.5, 39.2, 37.3, 36.1, 29.8, 28.0, 24.7, 22.7, 22.6, 19.7; IR (KBr) 3111, 2953, 2925, 2869, 1613, 1561, 1527, 1464, 1435, 1385, 1296, 1252, 1178, 1117, 1051 cm^{-1}; HRMS (FAB^+) calcd for $C_{63}H_{82}N_3O_6$ 976.6204 $[M + H]^+$, found 976.6221. Anal. Calcd for $C_{63}H_{81}N_3O_6$: C 77.50, H 8.36, N 4.30. Found: C 77.15, H 8.35, N 4.20%.

1,3,5-Tris{3-[(*S*)-4-(3,7-dimethyloctoxy)phenyl]isoxazol-5-yl}benzene *S*-5. To a solution of 1,3,5-triethynylbenzene (265 mg, 1.77 mmol) and benzohydroximoyl chloride *S*-**9** (1.82 mg, 5.84 mmol) in CH_2Cl_2 (20 mL) was added triethylamine (2.5 mL, 18 mmol). After stirring at room temperature for 48 h, the reaction mixture was concentrated. The crude product was purified by column chromatography on silica gel ($CHCl_3$) to give *S*-**5** (380 mg, 22%) as a white solid. Mp 140−141 °C; $[\alpha]^{25}_D$ = −5.9 $cm^3\ g^{-1}\ dm^{-1}$ (c 0.2 g cm^{-3} in chloroform); ^{1}H NMR (300 MHz, 10 mM, $CDCl_3$) δ 8.31 (s, 3H), 7.82 (d, J = 8.7 Hz, 6H), 7.01 (d, J = 8.7 Hz, 6H), 6.99 (s, 3H), 4.01−4.12 (m, 6H), 1.10−1.92 (m, 30H), 0.97 (d, J = 6.6 Hz, 9H), 0.88 (d, J = 6.6 Hz, 18H); ^{13}C NMR (75 MHz, 10 mM, $CDCl_3$) δ 168.1, 162.9, 160.8, 129.3, 128.2, 123.9, 120.9, 115.0, 98.8, 66.5, 39.2, 37.3, 36.1, 29.9, 28.0, 24.7, 22.7, 22.6, 19.7 ; IR (KBr) 3111, 2953, 2925, 2869, 1613, 1561, 1527, 1464, 1436, 1385, 1296, 1252, 1177, 1116, 1051 cm^{-1}; HRMS (FAB^+) calcd for $C_{63}H_{82}N_3O_6$ 976.6204 $[M + H]^+$, found 976.6223. Anal. Calcd for $C_{63}H_{81}N_3O_6$: C 77.50, H 8.36, N 4.30. Found: C 77.69, H 8.33, N 4.23%.

1,3,5-Tris{3-[4-(*tert*-butyldimethylsilyl)oxyphenyl]isoxazol-5-yl}benzene 11. To a solution of 1,3,5-triethynylbenzene (338 mg, 2.25 mmol), and benzohydroximoyl chloride **10**[30] (2.13 g, 7.45 mmol) in CH_2Cl_2 (40 mL) was added triethylamine (1.88 mL, 13.5 mmol). After stirring at room temperature for 48 h, the reaction mixture was concentrated. The crude product was purified by column chromatography on silica gel ($CHCl_3$) to give **11** (1.28 g, 63%) as a white solid. Mp 116−118 °C; ^{1}H NMR (300 MHz, 20 mM, $CDCl_3$) δ 8.31 (s, 3H), 7.78 (d, J = 8.7 Hz, 6H), 6.98 (s, 3H), 6.96 (d, J = 8.7 Hz, 6H), 1.01 (s, 27H), 0.26 (s, 18H); ^{13}C NMR (75 MHz, 20 mM, $CDCl_3$) δ 168.1, 163.0, 157.7, 129.3, 128.3, 124.0, 121.8, 120.7, 98.9, 25.6, 18.3, −4.4; IR (KBr) 2957, 2929, 2894, 2857, 1609, 1568, 1525, 1466, 1433, 1384, 1268, 1170, 1106, 1008 cm^{-1}; HRMS (FAB^+) calcd for $C_{51}H_{64}N_3O_6Si_3$ 898.4103 $[M + H]^+$, found 898.4123. Anal. Calcd for $C_{51}H_{63}N_3O_6Si_3$: C 68.19, H 7.07, N 4.68. Found: C 68.19, H 7.16, N 4.69%.

1,3,5-Tris[3-(4-dec-9-enyloxyphenyl)isoxazol-5-yl]benzene 2. To a solution of **11** (1.25 g, 1.50 mmol) in THF (15 mL) was added tetrabutylammonium fluoride (1.96 g, 7.50 mmol). After stirring at room temperature for 12 h, the reaction mixture was poured into aqueous NH_4Cl and extracted with EtOAc. The organic layer was dried over Na_2SO_4 and concentrated. Then, the crude product (510 mg) was dissolved in DMF (10 mL). 4-Dec-9-enyloxytoluene sulfonate[32] (1.09 g, 3.68 mmol) and K_2CO_3 (762 mg, 5.52 mmol) were added to the stirred solution. After refluxing for overnight, the reaction mixture was quenched with 1 N HCl. The resulting solution was extracted with EtOAc, dried over Na_2SO_4, and concentrated. The crude product was purified by column chromatography on silica gel (5% AcOEt/hexane) and GPC to give **2** (304 mg, 31%) as a white solid. Mp 114−115 °C; ^{1}H NMR (300 MHz, 30 mM, $CDCl_3$) δ 8.17 (s, 3H), 7.73 (d, J = 8.1 Hz, 6H), 6.94 (d, J = 8.1 Hz, 6H), 6.88 (s, 3H), 5.67−5.85 (m, 3H), 5.01 (ddt, J = 18, 1.2 Hz, 3H), 4.94 (ddt, J = 9.3, 1.2 Hz, 3H), 3.97 (t, J = 6.6 Hz, 6H), 2.06 (dt, J = 6.9, 6.6 Hz, 6H), 1.79 (m, 6H), 1.25−1.55 (m, 30H); ^{13}C NMR (75 MHz, 30 mM, $CDCl_3$) δ 167.9, 162.8, 160.8, 139.1, 129.1, 128.2, 123.7, 120.8, 114.8, 114.2, 98.7, 68.1, 33.8, 29.4 × 2, 29.2, 29.1, 28.9, 26.0; IR (KBr) 3115, 3074, 2924, 2851, 1639, 1612, 1562, 1526, 1466, 1436, 1387, 1295, 1251, 1176, 1115, 1020 cm^{-1}; HRMS (FAB^+) calcd for $C_{63}H_{76}N_3O_6$ 970.5734 $[M + H]^+$, found 970.5726. Anal. Calcd for $C_{63}H_{75}N_3O_6 \cdot H_2O$: C 76.56, H 7.85, N 4.25. Found: C 76.56, H 7.74, N 4.27%.

1,3,5-Tris[(4-decyloxyphenyl)-1-ethynyl]benzene 12. To a mixture of 1,3,5-tribromobenzene (800 mg, 2.54 mmol), (4-decyloxyphenyl)ethyne[33] (2.36 g, 8.66 mmol), and CuI (24 mg, 0.13 mmol) in Et_2NH (30 mL) was added $PdCl_2(PPh_3)_2$ (110 mg 0.157 mmol). After being stirred at 50 °C for 24 h, the reaction mixture was concentrated. The crude product was purified by column chromatography on silica gel (10% AcOEt/hexane) to give **12** (1.24 g, 58%) as a yellow solid. Mp 43−44 °C; ^{1}H NMR (500 MHz, 10 mM, $CDCl_3$) δ 7.57 (s, 3H), 7.45 (d, J = 8.9 Hz, 6H), 6.87 (d, J = 8.9 Hz, 6H), 3.97 (t, J = 6.6 Hz, 6H), 1.76−1.82 (m, 6H), 1.43−1.47 (m, 6H), 1.28−1.34 (m, 36H), 0.89 (t, J = 6.8 Hz, 9H); ^{13}C NMR (125 MHz, 10 mM, $CDCl_3$) δ 159.5, 133.4, 133.1, 124.3, 114.7, 114.6, 90.5, 86.7, 68.1, 31.9, 29.6, 29.5, 29.4, 29.3, 29.2, 26.0, 22.7, 14.1; IR (KBr) 3043, 2921, 2851, 2209, 1606, 1577, 1508, 1468, 1389, 1293, 1248, 1171, 1107, 1024 cm^{-1}; HRMS (FAB^+) calcd for $C_{60}H_{79}O_3$ 847.6029 $[M + H^+]$, found 847.6021. Anal. Calcd for $C_{60}H_{78}O_3$: C 85.06; H 9.28. Found: C 85.02; H 9.28%.

■ ASSOCIATED CONTENT

Supporting Information. TEM images of xerogel of **2**, florescence spectra, *T*-dependent plot, van't Hoff plots of **1**, chemical shift changes of the aromatic protons of **2**, **3**, and **5**, UV−vis absorption spectra of **12**, atomic coordinates of **13**, **14** and the hexameric assembly of **4**, and NMR spectra of all new compounds. This material is available free of charge via the Internet at http://pubs.acs.org.

■ AUTHOR INFORMATION

Corresponding Author

*E-mail: haino@sci.hiroshima-u.ac.jp.

■ ACKNOWLEDGMENT

This research work was supported by Grant-in-Aids for Scientific Research (Nos.18350065, 21350066) of JSPS, a Grant-in-Aid for Science Research (No.19022024) in a Priority Area "Super-Hierarchical Structures" from MEXT, Japan, and Yamada Science Foundation.

■ REFERENCES

(1) (a) Hoeben, F. J. M.; Jonkheijm, P.; Meijer, E. W.; Schenning, A. P. H. J. *Chem. Rev.* **2005**, *105*, 1491–1546. (b) Ariga, K.; Nakanishi, T.; Hill, J. P. *Curr. Opin. Colloid Interface Sci.* **2007**, *12*, 106–120. (c) Sada, K.; Takeuchi, M.; Fujita, N.; Numata, M.; Shinkai, S. *Chem. Soc. Rev.* **2007**, *36*, 415–435. (d) Ajayaghosh, A.; Praveen, V. K.; Vijayakumar, C. *Chem. Soc. Rev.* **2008**, *37*, 109–122. (e) Palmer, L. C.; Stupp, S. I. *Acc. Chem. Res.* **2008**, *41*, 1674–1684. (f) Praveen, V. K.; Babu, S. S.; Vijayakumar, C.; Varghese, R.; Ajayaghosh, A. *Bull. Chem. Soc. Jpn.* **2008**, *81*, 1196–1211. (g) Hasegawa, M.; Iyoda, M. *Chem. Soc. Rev.* **2010**, *39*, 2420–2427. (h) Hui, J. K. H.; MacLachlan, M. J. *Coord. Chem. Rev.* **2010**, *254*, 2363–2390.

(2) (a) Terech, P.; Weiss, R. G. *Chem. Rev.* **1997**, *97*, 3133–3159. (b) Shinkai, S.; Murata, K. *J. Mater. Chem.* **1998**, *8*, 485–495. (c) Abdallah, D. J.; Weiss, R. G. *Adv. Mater.* **2000**, *12*, 1237–1247. (d) van Esch, J. H.; Feringa, B. L. *Angew. Chem., Int. Ed.* **2000**, *39*, 2263–2266. (e) Gronwald, O.; Shinkai, S. *Chem.—Eur. J.* **2001**, *7*, 4328–4334. (f) George, M.; Weiss, R. G. *Acc. Chem. Res.* **2006**, *39*, 489–497.

(3) Hanabusa, K.; Okui, K.; Karaki, K.; Koyama, T.; Shirai, H. *J. Chem. Soc., Chem. Commun.* **1992**, 1371–1373.

(4) van Esch, J.; Schoonbeek, F.; de Loos, M.; Kooijman, H.; Spek, A. L.; Kellogg, R. M.; Feringa, B. L. *Chem.—Eur. J.* **1999**, *5*, 937–950.

(5) Yoza, K.; Ono, Y.; Yoshihara, K.; Akao, T.; Shinmori, H.; Takeuchi, M.; Shinkai, S.; Reinhoudt, D. N. *Chem. Commun.* **1998**, 907–908.

(6) Murata, K.; Aoki, M.; Suzuki, T.; Harada, T.; Kawabata, H.; Komori, T.; Ohseto, F.; Ueda, K.; Shinkai, S. *J. Am. Chem. Soc.* **1994**, *116*, 6664–6676.

(7) (a) Schenning, A. P. H. J.; Meijer, E. W. *Chem. Commun.* **2005**, 3245–3258. (b) Ajayaghosh, A.; Praveen, V. K. *Acc. Chem. Res.* **2007**, *40*, 644–656.

(8) Ishikawa, Y.; Kuwahara, H.; Kunitake, T. *J. Am. Chem. Soc.* **1994**, *116*, 5579–5591.

(9) Suzuki, M.; Yumoto, M.; Shirai, H.; Hanabusa, K. *Chem.—Eur. J.* **2008**, *14*, 2133–2144.

(10) (a) Messmore, B. W.; Hulvat, J. F.; Sone, E. D.; Stupp, S. I. *J. Am. Chem. Soc.* **2004**, *126*, 14452–14458. (b) Zang, L.; Che, Y.; Moore, J. S. *Acc. Chem. Res.* **2008**, *41*, 1596–1608. (c) Bhattacharya, S.; Samanta, S. K. *Langmuir* **2009**, *25*, 8378–8381. (d) Meijer, E. W.; De Greef, T. F. A.; Smulders, M. M. J.; Wolffs, M.; Schenning, A. P. H. J.; Sijbesma, R. P. *Chem. Rev.* **2009**, *109*, 5687–5754.

(11) (a) Ishi-i, T.; Shinkai, S. *Supramol. Dye Chem.* **2005**, *258*, 119–160. (b) Iyoda, M.; Hasegawa, M.; Enozawa, H. *Chem. Lett.* **2007**, *36*, 1402–1407.

(12) (a) Brotin, T.; Utermohlen, R.; Fages, F.; Bouaslaurent, H.; Desvergne, J. P. *J. Chem. Soc., Chem. Commun.* **1991**, 416–418. (b) Clavier, G.; Mistry, M.; Fages, F.; Pozzo, J. L. *Tetrahedron Lett.* **1999**, *40*, 9021–9024. (c) Mamiya, J.; Kanie, K.; Hiyama, T.; Ikeda, T.; Kato, T. *Chem. Commun.* **2002**, 1870–1871. (d) Würthner, F.; Yao, S.; Beginn, U. *Angew. Chem., Int. Ed.* **2003**, *42*, 3247–3250. (e) An, B. K.; Lee, D. S.; Lee, J. S.; Park, Y. S.; Song, H. S.; Park, S. Y. *J. Am. Chem. Soc.* **2004**, *126*, 10232–10233. (f) Morita, Y.; Tasaka, T.; Kawabe, K.; Okamoto, H.; Takenaka, S.; Kita, H. *Mol. Cryst. Liq. Cryst.* **2005**, *435*, 813–822.

(13) (a) Haino, T.; Tanaka, M.; Fukazawa, Y. *Chem. Commun.* **2008**, 468–470. (b) Haino, T.; Saito, H. *Synth. Met.* **2009**, *159*, 821–826.

(14) Haino, T.; Saito, H. *Aust. J. Chem.* **2010**, *63*, 640–645.

(15) Murata, K.; Aoki, M.; Nishi, T.; Ikeda, A.; Shinkai, S. *J. Chem. Soc., Chem. Commun.* **1991**, 1715–1718.

(16) John, G.; Jung, J. H.; Minamikawa, H.; Yoshida, K.; Shimizu, T. *Chem.—Eur. J.* **2002**, *8*, 5494–5500.

(17) (a) Baxter, N. J.; Williamson, M. P.; Lilley, T. H.; Haslam, E. *J. Chem. Soc., Faraday Trans.* **1996**, *92*, 231–234. (b) Martin, R. B. *Chem. Rev.* **1996**, *96*, 3043–3064. (c) Shetty, A. S.; Zhang, J. S.; Moore, J. S. *J. Am. Chem. Soc.* **1996**, *118*, 1019–1027. (d) Würthner, F.; Thalacker, C.; Diele, S.; Tschierske, C. *Chem.—Eur. J.* **2001**, *7*, 2245–2253. (e) Tobe, Y.; Utsumi, N.; Kawabata, K.; Nagano, A.; Adachi, K.; Araki, S.; Sonoda, M.; Hirose, K.; Naemura, K. *J. Am. Chem. Soc.* **2002**, *124*, 5350–5364. (f) Zhao, D. H.; Moore, J. S. *Org. Biomol. Chem.* **2003**, *1*, 3471–3491.

(18) Recently, Schenning and Meijer reported mechanistic insights into supramolecular polymerizations: Smulders, M. M. J.; Nieuwenhuizen, M. M. L.; de Greef, T. F. A.; van der Schoot, P.; Schenning, A. P. H. J.; Meijer, E. W. *Chem.—Eur. J.* **2010**, *16*, 362–367. Based on their report, the association mechanism of **1** was studied by using the UV/Vis absorption spectroscopy. Plots of the degree of aggregation, α_{agg}, vs T display a clear sigmoidal shape, indicating that the association obeys an isodesmic mechanism (Figure S2 in Supporting Information).

(19) Ishi-I, T.; Murakami, K. I.; Imai, Y.; Mataka, S. *J. Org. Chem.* **2006**, *71*, 5752–5760.

(20) Kastler, M.; Pisula, W.; Wasserfallen, D.; Pakula, T.; Mullen, K. *J. Am. Chem. Soc.* **2005**, *127*, 4286–4296.

(21) Ishi-i, T.; Kuwahara, R.; Takata, A.; Jeong, Y.; Sakurai, K.; Mataka, S. *Chem.—Eur. J.* **2006**, *12*, 763–776.

(22) Frisch, M. J.; Trucks, G. W.; Schlegel, H. B.; Scuseria, G. E.; Robb, M. A.; Cheeseman, J. R.; Montgomery, J. A.; Vreven, J. T.; Kudin, K. N.; Burant, J. C.; Millam, J. M.; Iyengar, S. S.; Tomasi, J.; Barone, V.; Mennucci, B.; Cossi, M.; Scalmani, G.; Rega, N.; Petersson, G. A.; Nakatsuji, H.; Hada, M.; Ehara, M.; Toyota, K.; Fukuda, R.; Hasegawa, J.; Ishida, M.; Nakajima, T.; Honda, Y.; Kitao, O.; Nakai, H.; Klene, M.; Li, X.; Knox, J. E.; Hratchian, H. P.; Cross, J. B.; Adamo, C.; Jaramillo, J.; Gomperts, R.; Stratmann, R. E.; Yazyev, O.; Austin, A. J.; Cammi, R.; Pomelli, C.; Ochterski, J. W.; Ayala, P. Y.; Morokuma, K.; Voth, G. A.; Salvador, P.; Dannenberg, J. J.; Zakrzewski, V. G.; Dapprich, S.; Daniels, A. D.; Strain, M. C.; Farkas, O.; Malick, D. K.; Rabuck, A. D.; Raghavachari, K.; Foresman, J. B.; Ortiz, J. V.; Cui, Q.; Baboul, A. G.; Clifford, S.; Cioslowski, J.; Stefanov, B. B.; Liu, G.; Liashenko, A.; Piskorz, P.; Komaromi, I.; Martin, R. L.; Fox, D. J.; Keith, T.; Al-Laham, M. A.; Peng, C. Y.; Nanayakkara, A.; Challacombe, M.; Gill, P. M. W.; Johnson, B.; Chen, W.; Wong, M. W.; Gonzalez, C.; Pople, J. A. *Gaussian 03*; Gaussian, Inc.: Wallingford, CT, 2004.

(23) Kolossvary, I.; Guida, W. C. *J. Am. Chem. Soc.* **1996**, *118*, 5011–5019.

(24) Mohamadi, F.; Richards, N. G. J.; Guida, W. C.; Liskamp, R.; Lipton, M.; Caufield, C.; Chang, G.; Hendrickson, T.; Still, W. C. *J. Comput. Chem.* **1990**, *11*, 440–467.

(25) Dehm, V.; Chen, Z. J.; Baumeister, U.; Prins, P.; Siebbeles, L. D. A.; Würthner, F. *Org. Lett.* **2007**, *9*, 1085–1088.

(26) Green, M. M.; Garetz, B. A.; Munoz, B.; Chang, H. P.; Hoke, S.; Cooks, R. G. *J. Am. Chem. Soc.* **1995**, *117*, 4181–4182.

(27) Yashima, E.; Maeda, K.; Nishimura, T. *Chem.—Eur. J.* **2004**, *10*, 42–51.

(28) (a) Jin, W.; Fukushima, T.; Niki, M.; Kosaka, A.; Ishii, N.; Aida, T. *Proc. Natl. Acad. Sci. U.S.A.* **2005**, *102*, 10801–10806. (b) van Gestel, J.; Palmans, A. R. A.; Titulaer, B.; Vekemans, J.; Meijer, E. W. *J. Am. Chem. Soc.* **2005**, *127*, 5490–5494. (c) Wilson, A. J.; van Gestel, J.; Sijbesma, R. P.; Meijer, E. W. *Chem. Commun.* **2006**, 4404–4406.

(29) (a) Green, M. M.; Reidy, M. P.; Johnson, R. J.; Darling, G.; Oleary, D. J.; Willson, G. *J. Am. Chem. Soc.* **1989**, *111*, 6452–6454. (b) Palmans, A. R. A.; Vekemans, J.; Havinga, E. E.; Meijer, E. W. *Angew. Chem., Int. Ed.* **1997**, *36*, 2648–2651. (c) Ajayaghosh, A.; Varghese, R.; George, S. J.; Vijayakumar, C. *Angew. Chem., Int. Ed.* **2006**, *45*, 1141–1144.

(30) Tanaka, M.; Haino, T.; Ideta, K.; Kubo, K.; Mori, A.; Fukazawa, Y. *Tetrahedron* **2006**, *63*, 652–665.

(31) Budzik, B. W.; Evans, K. A.; Wisnoski, D. D.; Jin, J.; Rivero, R. A.; Szewczyk, G. R.; Jayawickreme, C.; Moncol, D. L.; Yu, H. *Bioorg. Med. Chem. Lett.* **2010**, *20*, 1363–1367.

(32) Keith, C.; Reddy, R. A.; Hauser, A.; Baumeister, U.; Tschierske, C. *J. Am. Chem. Soc.* **2006**, *128*, 3051–3066.

(33) Lee, S. J.; Park, C. R.; Chang, J. Y. *Langmuir* **2004**, *20*, 9513–9519.